Supporting information

Bio-inspired synthesis of N-doped TiO_2/C nanocrystals by jellyfish mucus with high visible-light photocatalytic efficiency

Song Feng[a, b*], Lingchen Liu[c], Jianing Lin[d, e**], Ziwei Wang[f], Jinzeng Gu[d, e], Lutao Zhang[d, e], Bin Zhang[c**], Song Sun[a, b]**

[a]CAS Key Laboratory of Marine Ecology and Environmental Sciences, Institute of Oceanology, Chinese Academy of Sciences, Qingdao 266071, China

[b]College of Marine Science, University of Chinese Academy of Sciences, Qingdao, China

[c]School of Food and Biotechnology, Xihua University, Chengdu 610039, China

[d]Institute of Eco-Environmental Forensics, Shandong University, Qingdao 266237, China

[e]Laboratory for Marine Ecology and Environmental Science, Qingdao Marine Science and Technology Center, Qingdao 266237, China

[f]Liaoning University, Shenyang 110036, China

E-mail address for the first author: fengsong@qdio.ac.cn

**To whom correspondence should be addressed. E-mail: linjianing@sdu.edu.cn, lingchen2773@163.com, 0720060057@mail.xhu.edu.cn.

S1 Introduction

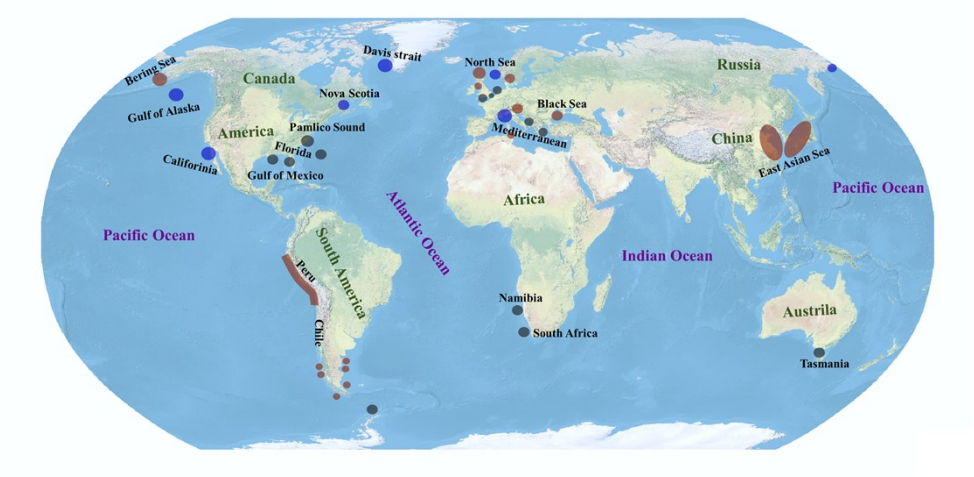

Fig. S1 Distribution of jellyfish blooms around the world. Colors indicate trends in jellyfish abundance over time by the end of 2011. Red sign: significant increase, blue sign: significant decrease, gray sign: no trend[1].

Fig. S2 Blooms of *Aurelia coerulea* and *Nemopilema nomurai* in the coastal sea of China and their damages. (a) Massive *A. coerulea* medusae (top right corner) bloomed inshore the Bohai, China. (b) *N. nomurai* medusae (top right corner) bloomed in large numbers in Bohai, Yellow and East China seas. (c) Massive aggregation of *A. coerulea* medusae by accident clogged the cooling water intakes seriously in a nuclear power plant, China, causing machine halt for approximately one week and economic loss of over 10 million RMB one day in July 2014[2]. (d) A serious clog of cooling water intakes (top right corner) by the massive aggregation of *A. coerulea* medusae appearing in the Qingdao power plant threatened the normal power supply of partial areas in July 2009[3]. (e) *N. nomurai* medusae massively appeared around some famous beaches, in Qin Huangdao, China in August, resulting in some stinging cases (top right corner)[4]. (f) Large amounts of *A. coerulea* ephyrae (top right corner) bloomed in many sea cucumber farming ponds constructed by artificial reefs in Dongying, China in spring, which have been regarded as the cause of sea cucumber vomiting (bottom right corner)[5].

Table S1 Some reports on the synthesis of C, N modified TiO_2 nanocrystals by the use of bioorganic matter from nature as nonmetal element sources.

Method	TiO_2 Precursor	Type of bioorganic matter	k (min^{-1})	Ref
Sol-gel and calcination	Tetrabutyl titanate (TBT)	Butterfly wings of *Papilio paris*	0.02614	6
Biomimetic template approach	TBT	Banana (*Musa acuminata*) stem fiber	0.0052	7
Biomimetic template approach	TBT	Polydopamine (PDA) spheres	—	8
Biomimetic template approach	Titanium trichloride	Lotus pollen	—	9
Hydrothermal method	TBT	Chicken feathers	0.0542	10
Biomimetic template approach	Titanium (IV) butoxide	Egg white protein	0.00669	11
Calcination	Titanium isopropoxide	*Ricinus Communis*, *Moringa Oleifera*, *Bougainvillea Spectabilis* plant extracts	—	12
Hydrothermal method	TBT	Extrapallial fluid of Fresh water mussels (*Cristaria plicata*)	—	13

k: the first order rate constant of C, N modified TiO_2 nanocrystals.

S2 Experimental section

S2.1 Extraction of jellyfish mucus proteins

Fresh medusae of *A. coerulea* and *N. nomurai* with the respective umbrella diameters of approximately 10~15 cm and 50~80 cm were captured in June and August in the coastal waters of Qingdao, China, respectively. The entire medusae in *A. coerulea* and partial oral arms in *N. nomurai* were rinsed thoroughly with fresh seawater filtered through a 0.45 μm hybrid fibre membrane, respectively. Afterwards, their mucus was collected into 50 mL centrifuges on ice by funnels containing a layer of medical gauze (Fig. S3). Then the obtained mucus was centrifuged at 4000~12000 rpm for 10 min to remove impurities. The supernatant was extracted by a disposable syringe.

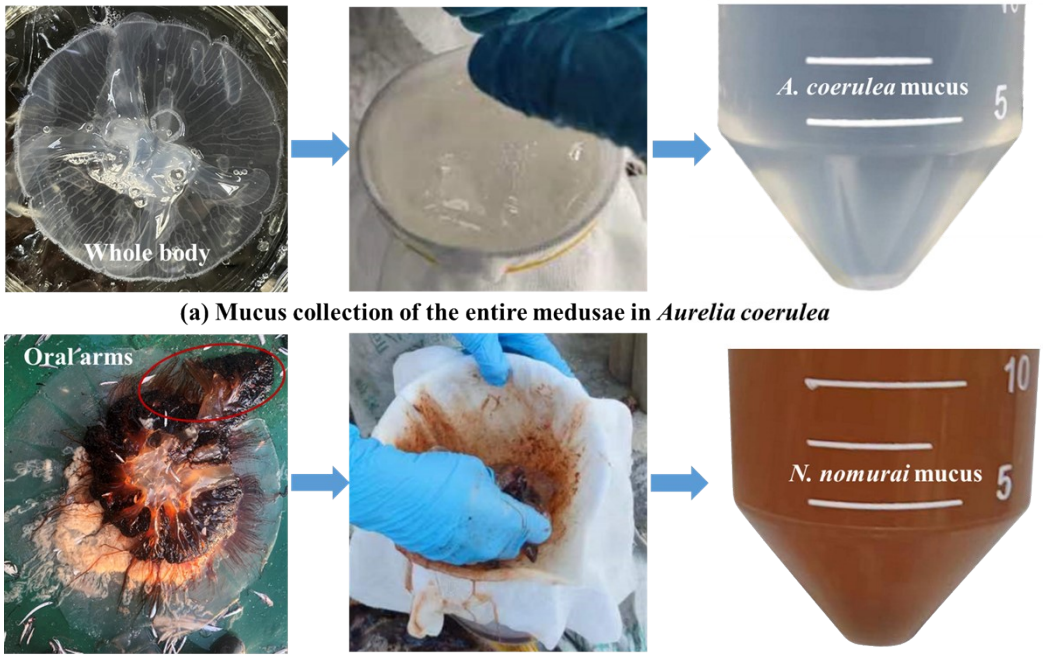

(a) Mucus collection of the entire medusae in *Aurelia coerulea*

(b) Mucus collection of partial oral arms in *Nemopilema nomurai*

Fig. S3 Mucus collection of the entire medusae in *Aurelia coerulea* (a) and partial oral arms in *Nemopilema nomurai* (b)

S2.2 Analysis of jellyfish mucus proteins

The protein concentration of *A. coerulea* and *N. nomurai* mucus was determined using the

Bradford Assay (Bradford, 1976). The proteins in the mucus were detected by 10% sodium dodecyl sulphate-polyacrylamide gel electrophoresis (SDS-PAGE). For sample preparation, jellyfish mucus proteins were mixed with SDS-PAGE protein loading buffer (5×) at a ratio of 4 μL to 1 μL. The mixture was then heated to 100°C for 5 min to ensure proper denaturation of the proteins. Subsequently, 30 μL of the prepared mixture was added to each sampling well in the gel. The gel was subjected to electrophoresis at a voltage of 80 v using the electrophoresis apparatus. After electrophoresis, the gel was stained with Commassie Blue Fast Staining Solution and photographed after 5 min.

The standard curves of proteins were determined as follows. The various volumes (i.e., 0, 3, 5, 7, and 9 μL) of Bovine Serum Albumin (BSA) standard liquid (1 $mg \bullet mL^{-1}$) were added to 96-well plates, which were supplemented with PBS buffer solution to 10 μL. After uniform mixing, 200 μL Commassie Blue G250 staining solution was added to each well. The absorbance of samples was measured at 595 nm by a microplate reader (MD VersaMax) after being mixed for 30 s and then left at room temperature for 5 min. The standard curves of sample proteins were finally obtained in Fig. S4. The horizontal coordinate (x) represented the absorbance, and the vertical coordinates (y) represented the protein concentration (μg/L). The corresponding linear regression equation was described as follows:

$$y=1611.08101x-892.57658,\ R^2=0.999 \quad (1)$$

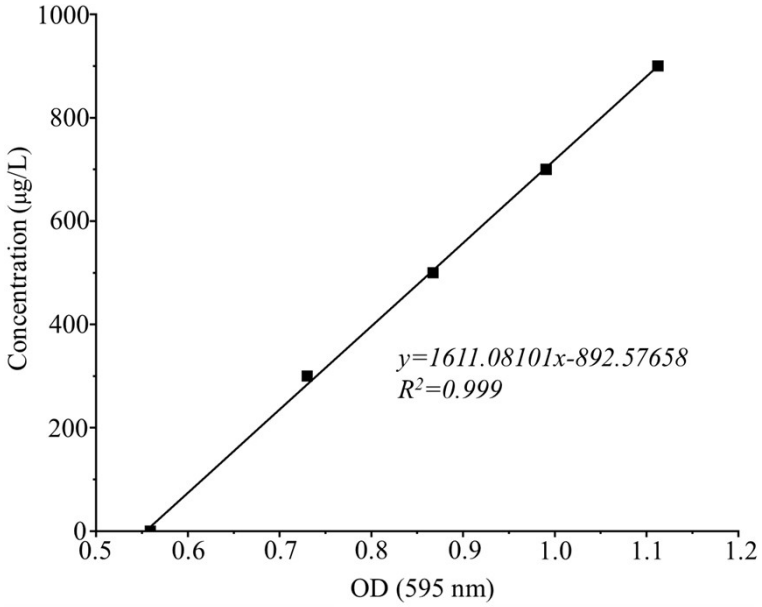

84

85 **Fig. S4** Standard curve of Bovine Serum Albumin (BSA)

86 The mucus protein concentration of *A. coerulea* and *N. nomurai* were eventually calculated
87 based on the linear regression equation by sampling 10 μL. The mucus proteins were finally diluted
88 or concentrated to the designed concentration (600 $\mu g \cdot mL^{-1}$) as the dopants for the synthesis of the
89 modified TiO_2 nanocrystals by referring to the reports of Zeng et al. (2015)[13].

90 **S2.3 Synthesis of TiO_2 materials**

91 The schematic of the synthetic process of modified TiO_2 nanocrystals by using proteins of *A.*
92 *coerulea* and *N. nomurai* mucus as dopants was described in Fig. 1. Three volumes of mucus
93 proteins (10 mL, 20 mL and 30 mL) in *A. coerulea* and *N. nomurai*, were separately added to 5 mL
94 of tetrabutyl titanate (TBT, 97%, Sigma-Aldrich) in a 50 mL beaker with the volume ratios of 2:1,
95 4:1 and 6:1. They were constantly stirred for 2 h at 300 $rpm \cdot min^{-1}$. After 4h mineralization without
96 stirring, the mixture (i.e., jellyfish mucus and TBT) was transferred to a Teflon-lined autoclave and
97 preheated at 50°C for 30 min. Then temperature was adjusted to 150°C at a heating rate of
98 $5°C \cdot min^{-1}$. The heat treatment process at 150°C lasted for 12 h. When the reactor naturally cooled

to the room temperature, the mixture containing the light brown precipitate and liquid appeared (Fig. S5a). Afterwards, the precipitate was collected by firstly centrifugation at 4000 rpm•min^{-1} for 10 min, followed by separately washed with anhydrous ethanol and distilled water for 3 times, and dried at 55°C for 12 h. The modified TiO_2 nanocrystals were finally obtained after thorough grinding (Fig. S5b), which were denoted as JAT for *A. coerulea* and JNT for *N. nomurai*, respectively. According to the volume ratio between their mucus proteins utilized and TBT, the 6 TiO_2 nanocrystals were abbreviated as JAT-2, JAT-4, and JAT-6, as well as JNT-2, JNT-4, and JNT-6, respectively.

Fig. S5 Light brown precipitate and liquid after hydrothermal treatment (a) and eventually prepared modified TiO_2 nanocrystals (b) after grinding by using *N. nomurai* mucus as the dopants.

S2.4 Characterization of materials

The morphology of the obtained modified TiO_2 samples was characterized by the scanning electron microscopy (SEM, TESCAN MIRA LMS) and transmission electron microscopy (TEM, JEOL JEM 2100F). For SEM, the sample could be directly observed on the sample table with conductive adhesive. For TEM, the sample was firstly ultrasonic dispersed in anhydrous ethanol to form a uniform solution, and then dropped onto a micro-grid copper net for observation. The crystalline phase was analyzed by X-ray diffraction (XRD, Rigaku SmartLab SE) with Cu-Kα radiation (operation voltage of 40 kV and current of 40 mA). The scan was collected between 10 and 80 degrees at the scanning rate of 2 °/min. The nitrogen adsorption-desorption isotherms were

measured by an automatic adsorption unit (Quantachrome Autosorb IQ) at 196°C after degassing of samples for 8 h. The pore surface, volume and diameter distribution were determined by Barrett-Joyner-Halenda (BJH) method. The X-ray photoelectron spectroscopy (XPS, Thermo Scientific K-Alpha) was used to determine the surface element composition, chemical bonding valence states, and charge distribution of the sample. The UV-vis absorption spectra of the samples were measured by Shimadzu UV-3600i Plus equipped with an integrating sphere attachment, using $BaSO_4$ as the reference in the wavelength range of 200~800 nm. Photoluminescence (PL) spectra were obtained (Edinburgh FLS1000) with a 300~700 nm excitation wavelength to reveal the process of separation, migration and recombination of photogenerated electron-hole and compare the lifetime of photogenerated carrier. The active radicals during the photocatalytic reaction process were identified using electron paramagnetic resonance spectrometer (ESR, Bruker EMXplus-6/1) at the magnetic field strength of 3510G. Electrochemical impedance spectroscopy (EIS) was analyzed using CHI760E. The photocatalyst was dispersed in 1 mL of ultrapure water solution and then 50 μL nafion solution was added. The uniform suspension was formed by ultrasonication for 30 min. Afterwards, 150 μL of suspension was added onto ITO glass and dried at room temperature for optoelectronic test at the CHI760E electrochemical workstation. The Ag/AgCl was the reference electrode, and the Pt wire was the contrast electrode. Each photocatalyst was the working electrode, and the electrolyte was 0.5 $mol \cdot L^{-1}$ potassium ferricyanide solution. The EIS frequency was 0.1~100 Khz. The radius of EIS curve impedance can reflect the conductivity of photocatalyst.

S2.5 Photocatalytic activity measurement

The photocatalytic activity of the samples was evaluated by the degradation of Rhodamine B (RhB) dye under visible-light irradiation. The 500 W mercury lamp equipped with 400 nm filter

was used as a light source. 10 mg samples were added into 10 mL RhB (0.01 mM) aqueous solution. After the solution was stirred for 30 min in the dark, it was exposed to the visible light. 1 mL solution was taken out by pipettes every 5 min, and the supernatant was obtained by centrifugation. The concentration of the degradation solution was determined by the absorbance at 554 nm using a microplate reader. The degradation rates (D, %) of RhB were calculated as follows Eq. (1):

$$D=(C_0-C_t)/C_0\times100\% \quad (2)$$

where C_0 (mmol/L) is the initial RhB concentration (ppm), and C_t (mmol/L) is the RhB concentration at time t.

In order to better evaluate the reusability and stability of prepared photocatalysts, cyclic experiments were conducted. After each cycle experiment, the photocatalyst was repeatedly washed with ultrapure water and anhydrous ethanol, and then placed in a beaker and boiled with ultrapure water to remove residual organic molecules. Subsequently, the photocatalyst was dried at 60℃, and the above experiment was repeated three times.

Table S2 Experimental apparatus used in this study

Instrument name	Instrument model	Manufacturer
Photochemical reaction apparatus	BA-GHX1	Bayue Instrument Co., Ltd, Changsha, China
Muffle furnace	HAD-TE0912	Heng odd Instrument Co., Ltd, Beijing, China
Electro-thermostatic blast oven	DHG-9245A	Yiheng17 Instrument Co., Ltd, Shanghai, China
Heating Magnetic Stirrer	HJ-6A	Guohua Instrument Co., Ltd, Changzhou, China
Microplate reader	MD VersaMax	Molecular Devices
Electrophoresis apparatus	JY-CZ-B	Junyi Electrophoresis Ltd, Beijing, China
Ultrapure water machine	RODI-220A	ResearchScientific Instruments Co., Ltd, Xiamen, China
Ultrasonic cleaners	KQ-300E	Supmile Instruments Co., Ltd,

		Kunshan, China
Refrigerated centrifuge	Centrifuge 5810R	Eppendorf Co., Ltd, Germany
Turbine mixer	VM-500S	Joanlab Co., Ltd, Huzhou, China
Analytical balance	BAS2245-CW	Sartorius Co., Ltd, Germany
X-ray diffractometer	Rigaku SmartLab SE	Rigaku Co., Ltd, Japan
SEM	TESCAN MIRA LMS	Tescan Co., Ltd, Czech Republic
TEM	JEOL JEM 2100F	Rigaku Co., Ltd, Japan
Automatic surface and porosity analyzer	Quantachrome Autosorb IQ	Quantachrome Co., Ltd, USA
X-ray photoelectron spectroscopy	Thermo Scientific K-Alpha	Thermo Fisher Scientific Co., Ltd, USA
UV-vis spectrophotometer	Shimadzu UV-3600i Plus	Shimadzu Co., Ltd, Japan
Fluorescence spectrophotometer	Edinburgh FLS1000	Edinburgh Co., Ltd, UK
Electron Paramagnetic Resonance Spectrometer	Bruker EMXplus-6/1	Bruker Co., Ltd, Germany

S3 Results and discussions

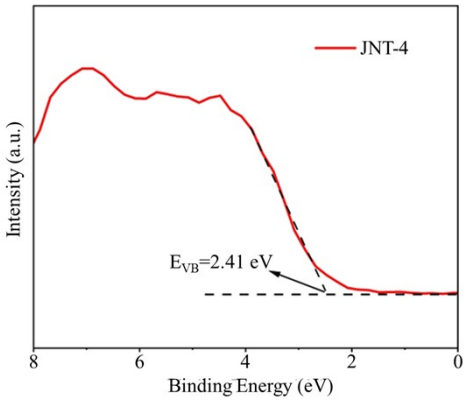

Fig. S6 XPS valence band spectra of JNT-4 nanocrystal.

References

1 R. H. Condon, C. M. Duarte, K. A. Pitt, K. L. Robinson, C. H. Lucas, K. R. Sutherland, H. W. Mianzan, M. Bogeberg, J. E. Purcell, M. B. Decker, S. Uye, L. P. Madin, R. D. Brodeur, S. H. D. Haddock, A. Malej, G. D. Parry, E. Eriksen, J. Quinones, M. Acha, M. Harvey, J. M. Arthur and W. M. Graham, Recurrent jellyfish blooms are a consequence of global oscillations, *P. Natl Acad. Sci. USA*, 2013, **110**, 1000-1005.

2 J. Li, X. Liu, J. Zhang and Y. Meng, Research on marine biological detection technology to improve the safety of cooling water source in nuclear power plants, *Electrical. Secur.*, 2017, **10**, 32-37 (in Chinese).

3 L. Ren, Jellyfish attacked on a power plant in Qingdao possibly resulting in the shutdown or affecting the power supply of 1/3 areas, *Qingdao News*, 2009, 7-8. (in Chinese).

4 S. Feng, S. Sun, C. Li and F. Zhang, Controls of *Aurelia coerulea* and *Nemopilema nomurai* (Cnidaria: Scyphozoa) blooms in the coastal sea of China: Strategies and measures, *Front. Mar. Sci.*, 2022, **9**, 946830.

5 Z. Dong, Blooms of the moon jellyfish Aurelia: Causes, consequences and controls, *World seas: An environmental evaluation: Volume III: Ecological issues and environmental impacts*, 2019, 163-170.

6 J. Li, L. Gao and W. Gan, Bioinspired C/TiO_2 photocatalyst for rhodamine B degradation under visible light irradiation, *Front. Agr. Sci. Eng.*, 2017, **4**, 459-464.

7 R. Purbia, R. Borah and S. Paria, Carbon-doped mesoporous anatase TiO_2 multi-tubes nanostructures for highly improved visible light photocatalytic activity, *Inorg. Chem.*, 2017, **56**, 10107-10116.

8 Y. Huang, K. Chen, M. Huang, R. Bi, Z. Li, Y. Zhu, M. Tang, Z. Tong, Y. Ye and M. Zhu, Versatile polydopamine-mediated growth of N and C co-doped hollow porous TiO_2 spheres with oxygen vacancies for visible-light-driven oxidation of acetaldehyde, *J. Environ. Chem. Eng.*, 2023, **11**, 110887.

9 X. Jiang, J. Zhou, H. Liu, Y. Chen and C. Lu, Lotus pollen-templated synthesis of C, N, P-self doped $KTi_2(PO4)_3/TiO_2$ for sodium ion battery, *Colloids Surface. A.*, 2022, **650**, 129605.

10 G. Zhu, X. Yang, Y. Liu, Y. Zeng, T. Wang and H. Yu, One-pot synthesis of C-modified and N-doped TiO_2 for enhanced visible-light photocatalytic activity, *J. Alloy. Compd.*, 2022, **902**, 163677.

11 A. N. Kadam, T. T. Salunkhe, H. Kim and S. W. Lee, Biogenic synthesis of mesoporous N-S-C tri-doped TiO_2 photocatalyst via ultrasonic-assisted derivatization of biotemplate from expired egg white protein, *Appl. Surf. Sci.*, 2020, **518**, 146194.

12 J. López-Mercado, M. I. González-Dominguez, F. J. Reynoso-Marin, B. Acosta, E. Smolentseva and A. Nambo. Green synthesis of TiO_2 for furfural production by photohydrolysis of tortilla manufacturing waste, *Sci. Rep-UK*, 2023, **13**, 15355.

13 H. Zeng, J. Xie, H. Xie, B.L. Su, M. Wang, H. Ping, W. Wang, H. Wang and Z. Fu, Bioprocess-inspired synthesis of hierarchically porous nitrogen-doped TiO_2 with high visible-light photocatalytic activity, *J. Mater. Chem. A*, 2015, **3**, 19588-19596.